Electron-positron enhancement factors at a metal surface: Aluminum

Anna Rubaszek
W. Trzebiatowski Institute of Low Temperature and Structure Research, Polish Academy of Sciences, P.O. Box 937, 50-950 Wrocław 2, Poland
(Received 20 November 1990; revised manuscript received 26 July 1991)

Momentum density of annihilating electron-positron pairs at an Al surface is calculated within an approximation developed by the author. The surface momentum-dependent enhancement factor is investigated. This parameter is found to be a decreasing function of momentum for a clean Al surface, in spite of its behavior in the bulk metal.

I. INTRODUCTION

Interest in slow positron interactions with metal surfaces has increased in the past few years.[1] Particularly, the well-known angular correlation of annihilation radiation (ACAR) technique[2] has been successfully applied to investigations of electron and positron surface states in Al,[3,4] Cu,[5] Si,[4,6] Ni,[4,7] Pb,[8] and graphite.[9]

The interpretation of ACAR data in terms of the electronic structure of metallic systems is based on the belief that positron annihilation yields information about one-electron states of the material. A series of slow-positron experiments performed recently on various metal surfaces[3-10] produced some surprising results from the point of view of positron-annihilation characteristics in the bulk. One of them is the lifetime of the positron surface state (SS) which amounts to 580 psec for the Al(110) surface,[10] i.e., about 15% more than the spin-averaged free-positronium (Ps) value. Furthermore, unlike the ACAR spectrum from the Cu(121) face[5] (which displays a strong anisotropy, in agreement with theoretical expectations), the surface-state components of the two-dimensional (2D) ACAR spectra for any of three low-index surfaces of Al [(100), (110), and (111)] are nearly isotropic and face independent.[4] In contrast to the surface state, the momentum density of the positronium emission from Al depends appreciably on the crystal orientation, and in the Al(110) spectrum a clear anisotropy occurs.[4] The discrepancies between experimental[4,10] and theoretical[11-15] annihilation characteristics (cf. discussion in Ref. 4) indicate that in the calculations of the SS annihilation parameters both the individual electronic-state distributions and electron-positron correlations must be treated very carefully.

First of all, the theoretical results for the SS ACAR spectra are as reliable as the electron wave functions used in the description of the unperturbed material are correct,[2] at least for the region where the positron is found. For this reason the mixed-density approximation[12] (which assumes the electron wave functions in the form of single plane waves filling the Fermi sphere of local Fermi radius) is invalid in the surface region, and conclusions about the shape of the SS ACAR spectra drawn within the approach of Ref. 12 turned out to be misleading, as pointed out in Refs. 15 and 16.

A proper treatment of electron-positron correlations at the surface is very important.[12-20] When the enhancement of electron density on the positron is neglected,[11,12] the SS lifetime for an Al surface is one order of magnitude longer than the experimental one,[10] as shown in Ref. 15. The local-density approximation[13,15,18-20] (LDA) approach should also be modified when the SS annihilation characteristics are calculated. Treating the electron screening cloud as in a jellium of local electron density[12,13,15,21,22] leads to a positron SS lifetime τ which never exceeds the free-Ps value of 500 psec. Moreover, the SS ACAR spectra calculated within the LDA (Ref. 15) are too narrow; the electron-positron correlation potential obtained within the LDA tends to the constant value of 0.25 atomic units (see the dependence of the correlation potential on the electron density in jellium, parametrized by Boroński and Nieminen[23(d)]), instead of reproducing the correct image form, which had to be imposed.[12,13,15]

The shape of the positron wave function has a crucial effect on the resulting SS positron-annihilation characteristics.[12,13] There has been considerable theoretical effort devoted to modeling the positron in the surface state.[1] The positron distribution at the surface is strongly dependent on the background electron charge density as well as on the electron-positron correlation potential. Here the density-functional formalism[18,23-25] and the Feynman theorem[18,24,26] or electric-field approach[27] seem to be useful starting points for the treatment of the problem. The form of the potential acting on the positron at the surface and the change in the electron density on the positron site, due to the electron-positron interaction, cannot be considered separately (as, e.g., in Refs. 11-13) in the calculations of the positron SS annihilation characteristics. The problem of electron-positron correlations should be treated on a broad basis in a consistent way.

The aim of the present work is to study the effect of electron-positron correlations on the surface-state positron-annihilation characteristics. An approximation proposed in Ref. 16 is used to obtain SS ACAR spectra from an Al surface. The background electron charge density, positron distribution, and electron-positron correlations are treated in common in the calculations of positron-annihilation characteristics. In this context the applicability of the independent-particle model (IPM) to

the surface problem is discussed. The momentum dependence of the electron-positron enhancement factors at an Al surface is investigated. Although the calculations are performed within the jellium model of an Al surface, nevertheless, the proposed formalism is general, and it can be applied to the calculation of SS positron lifetime and ACAR spectra for a more realistic discrete-lattice model of any metal surface, based only on the values of the individual electron wave functions in the material investigated.

II. FORMALISM

The 2D ACAR slow-positron experiment measures the 2D projections of 3D momentum density (MD) of an initial state of the one-positron many-electron system or of the Ps atom formed and emitted from the surface. The surface-state part of the momentum distribution of annihilating pairs, $\rho(\mathbf{p})$, is given by the expression

$$\rho(\mathbf{p})=\sum_{i_{\mathrm{occ}}}\left|\int e^{-i\mathbf{p}\cdot\mathbf{r}}\psi_i^{ep}(\mathbf{r},\mathbf{r})d\mathbf{r}\right|^2 , \tag{1a}$$

where $\mathbf{p}=(p_x,p_y,p_z)$ is the annihilation photon-pair momentum and $\psi_i^{ep}(\mathbf{r}_e,\mathbf{r}_p)$ are the pair wave functions of the thermalized positron located at $\mathbf{r}_p$ and electron in the initial state i located at $\mathbf{r}_e$. The summation in Eq. (1a) is over all occupied electronic states i. The corresponding 2D SS ACAR spectra can be expressed as

$$N_{\mathrm{SS}}(p_x,p_z)=\xi\int\rho(\mathbf{p})dp_y ,$$

where p_z is assumed to be normal to the surface and ξ is a normalization constant, generally dependent on the geometry of experiment, intensity of the source, positron lifetime τ, and time duration of the experiment. The long-slit (1D) ACAR spectra can be generated from the 2D spectrum by the integrations

$$N(p_z)=\int N_{\mathrm{SS}}(p_x,p_z)dp_x ,$$

$$N(p_x)=\int N_{\mathrm{SS}}(p_x,p_z)dp_z .$$

The total annihilation rate λ ($\lambda=1/\tau$) for the positron in the surface state is related to $\rho(\mathbf{p})$ according to the formula [cf. also Eq. (1a)]

$$\lambda=\frac{\pi r_0^2 c}{(2\pi)^3}\int d\mathbf{p}\,\rho(\mathbf{p})=\pi r_0^2 c\int d\mathbf{r}\left[\sum_{i_{\mathrm{occ}}}|\psi_i^{ep}(\mathbf{r},\mathbf{r})|^2\right] , \tag{1b}$$

where r_0 and c are the classical electron radius and velocity of light, respectively.

It should be pointed out that the case of metal-surface calculations of $\psi_i^{ep}(\mathbf{r}_e,\mathbf{r}_p)$ is fairly more complicated than that for a bulk metal. First of all, the standard band-structure methods of determining the unperturbed electron wave functions in the material investigated (in the absence of a positron), $\psi_i^0(\mathbf{r}_e)$, are to be modified, as the periodicity conditions are violated in the direction perpendicular to the surface. The next point is connected with electron-positron correlations, which influence both the shape of a positron wave function $\psi_+(\mathbf{r}_p)$ (as is shown in Sec. II A) and change the density of individual electronic states on the positron position.[12,13,15–22,23(d)] In order to inspect this problem, it is convenient to introduce the conditional electron wave functions and conditional density of the electronic charge screening the positron, assuming that the positron is located at $\mathbf{r}_p$, $\psi_i(\mathbf{r}_e;\mathbf{r}_p)$, and $\Delta\rho(\mathbf{r}_e;\mathbf{r}_p)$, respectively, according to the formulas

$$\psi_i(\mathbf{r}_e;\mathbf{r}_p)=\psi_i^{ep}(\mathbf{r}_e,\mathbf{r}_p)/\psi_+(\mathbf{r}_p)$$

and

$$\Delta\rho(\mathbf{r}_e;\mathbf{r}_p)=\sum_{i_{\mathrm{occ}}}|\psi_i(\mathbf{r}_e;\mathbf{r}_p)|^2-n_{\mathrm{el}}(\mathbf{r}_e) . \tag{2a}$$

Here

$$n_{\mathrm{el}}(\mathbf{r}_e)=\sum_{i_{\mathrm{occ}}}|\psi_i^0(\mathbf{r}_e)|^2 \tag{2b}$$

is the local electron density in the unperturbed material. The screening charge distribution $\Delta\rho(\mathbf{r}_e;\mathbf{r}_p)$ for any $\mathbf{r}_p$ should satisfy the charge-neutrality condition

$$\int\Delta\rho(\mathbf{r}_e;\mathbf{r}_p)d\mathbf{r}_e=1 . \tag{2c}$$

In terms of the conditional wave functions and screening charge density [Eq. (2a)], formulas (1a) and (1b) take the form

$$\rho(\mathbf{p})=\sum_{i_{\mathrm{occ}}}\left|\int e^{-i\mathbf{p}\cdot\mathbf{r}}\psi_+(\mathbf{r})\psi_i(\mathbf{r};\mathbf{r})d\mathbf{r}\right|^2$$
$$=\sum_{i_{\mathrm{occ}}}\left|\int e^{-i\mathbf{p}\cdot\mathbf{r}}\psi_+(\mathbf{r})\psi_i^0(\mathbf{r})\sqrt{f(\mathbf{r},i)}d\mathbf{r}\right|^2 \tag{3a}$$

and

$$\lambda=\pi r_0^2 c\int d\mathbf{r}|\psi_+(\mathbf{r})|^2\left[\sum_{i_{\mathrm{occ}}}|\psi_i(\mathbf{r};\mathbf{r})|^2\right]$$
$$=\pi r_0^2 c\int d\mathbf{r}|\psi_+(\mathbf{r})|^2 n_{\mathrm{el}}(\mathbf{r})\left[1+\frac{\Delta\rho(\mathbf{r};\mathbf{r})}{n_{\mathrm{el}}(\mathbf{r})}\right] , \tag{3b}$$

where the two-particle enhancement functions $f(\mathbf{r},i)$ are defined as (cf. Refs. 15, 16, and 19–22)

$$f(\mathbf{r},i)=|\psi_i(\mathbf{r};\mathbf{r})|^2/|\psi_i^0(\mathbf{r})|^2 .$$

Each of the functions $f(\mathbf{r}_p,i)$, as well as the function

$$F(\mathbf{r}_p)=1+\Delta\rho(\mathbf{r}_p;\mathbf{r}_p)/n_{\mathrm{el}}(\mathbf{r}_p) ,$$

has a definite physical meaning: $f(\mathbf{r}_p,i)$ describes the enhancement of the density of the electronic state i on the positron site from its initial value $|\psi_i^0(\mathbf{r}_p)|^2$, under the condition that the positron is located at $\mathbf{r}_p$, while $F(\mathbf{r}_p)$ corresponds to the change of the total electron density on the positron position. The enhancement of the local electron density, $F(\mathbf{r})=1+\Delta\rho(\mathbf{r};\mathbf{r})/n_{\mathrm{el}}(\mathbf{r})$, used in the formula (3b), is, according to Eq. (2a), equal to the weighted average of individual electron-positron enhancements $f(\mathbf{r},i)$ [cf. the ACAR formula (3a)] over states i, i.e.,

$$F(\mathbf{r})=1+\frac{\Delta\rho(\mathbf{r};\mathbf{r})}{n_{\mathrm{el}}(\mathbf{r})}=\frac{1}{n_{\mathrm{el}}(\mathbf{r})}\sum_{i_{\mathrm{occ}}}|\psi_i^0(\mathbf{r})|^2 f(\mathbf{r},i)$$
$$=\langle f(\mathbf{r},i)\rangle_i \ . \tag{4}$$

If the functions $f(\mathbf{r},i)$ were state independent [i.e., $f(\mathbf{r},i)\equiv f(\mathbf{r})$], they would be exactly equal to $F(\mathbf{r})=1+\Delta\rho(\mathbf{r};\mathbf{r})/n_{\mathrm{el}}(\mathbf{r})$ according to Eqs. (2b) and (4).

It should be stressed here that the theoretical prediction of two-particle correlations $f(\mathbf{r},i)$ for separate electronic states i at the surface is very complicated and, up to date, has not been performed. Fortunately, as shown later in this work, the momentum dependence of $f(\mathbf{r},i)$ is much less pronounced in the region where the positron is found than their position dependence. Thus the functions $f(\mathbf{r},i)$ in the ACAR formula (3a) can be approximated by their average over i, $F(\mathbf{r})$ [Eq. (4)]. This leads to the new ACAR formula[16]

$$\rho(\mathbf{p})=\sum_{i_{\mathrm{occ}}}\left|\int e^{-i\mathbf{p}\cdot\mathbf{r}}\psi_+(\mathbf{r})\psi_i^0(\mathbf{r})\left[1+\frac{\Delta\rho(\mathbf{r};\mathbf{r})}{n_{\mathrm{el}}(\mathbf{r})}\right]^{1/2}d\mathbf{r}\right|^2 , \tag{5}$$

used in the present work in calculations of positron SS annihilation characteristics.

Closer inspection of Eqs. (2a), (3b), and (5) leads to the conclusion that the positron-annihilation characteristics are well determined by the wave functions of individual electronic states in the host material, $\psi_i^0(\mathbf{r})$, and the electronic screening charge distribution, $\Delta\rho(\mathbf{r}_e;\mathbf{r}_p)$. As shown in Sec. II A (cf. also Ref. 20), the positron wave function appearing in formulas (3b) and (5) is generated by the above quantities and it cannot be considered separately, as independent of $\Delta\rho(\mathbf{r}_e;\mathbf{r}_p)$ (as in Refs. 11–13).

A. Influence of the background electron charge density and electron-positron correlations on the positron distribution at the surface

The positron and unperturbed electron wave functions at the surface may be found using a standard density-functional method.[18,23–25] The electron wave functions ψ_i^0 obtained within the Hohenberg-Kohn-Sham[23(a),23(b)] (HKS) formalism are the solutions of the set of one-particle Schrödinger equations[11,12,15,19,20] (atomic units are used throughout)

$$[-\tfrac{1}{2}\nabla_e^2+V_{\mathrm{eff}}(\mathbf{r}_e)]\psi_i^0(\mathbf{r}_e)=E_i\psi_i^0(\mathbf{r}_e) \ , \tag{6a}$$

where $V_{\mathrm{eff}}(\mathbf{r}_e)=V_C(\mathbf{r}_e)+V_{\mathrm{xc}}(\mathbf{r}_e)$ is the electron potential, consisting of the electrostatic Hartree (V_C) and electron-electron exchange-correlation (V_{xc}) parts, and E_i denote the electron energy eigenvalues. The Coulomb potential $V_C(\mathbf{r})$ and electron-density profile $n_{\mathrm{el}}(\mathbf{r})$ generate each other, according to Eqs. (2b), (6a), and the Poisson equation.

The positron wave function is an eigenfunction of the equation

$$[-\tfrac{1}{2}\nabla_p^2+V_+(\mathbf{r}_p)]\psi_+(\mathbf{r}_p)=E_+\psi_+(\mathbf{r}_p) \ , \tag{6b}$$

where E_+ is the positron ground-state energy and the positron potential $V_+(\mathbf{r}_p)=-V_C(\mathbf{r}_p)+V_{\mathrm{corr}}(\mathbf{r}_p)$ is the sum of the electron Hartree (with opposite sign) and electron-positron correlation potentials $-V_C$ and V_{corr}, respectively.[11,15,18,20,23(c),23(d)] As shown schematically in Fig. 1, the repulsive Coulomb potential $-V_C(\mathbf{r}_p)$ repels a positron from the metal to the vacuum, while the attractive correlation potential, because of the existence of the electronic cloud screening the positron [$\Delta\rho(\mathbf{r}_e;\mathbf{r}_p)\not\equiv 0$], causes trapping of the positron at the surface, preventing it from escaping far outside the metal (the corresponding effective electron potential V_{eff} is presented in Fig. 2 of Ref. 15). The Coulomb part of the potential experienced by the positron [$-V_C(\mathbf{r})$] is determined by the background electron charge density $n_{\mathrm{el}}(\mathbf{r})$.

Since the positron distorts the background electron charge density, the correlation potential $V_{\mathrm{corr}}(\mathbf{r}_p)$ should be thought of as the work done to bring the positron to $\mathbf{r}_p$ against the Coulomb forces between the positron and electronic polarization cloud. There are several ways of taking into account nonstatic effects in the calculation of V_{corr} on the basis of the exact form of screening charge distribution $\Delta\rho(\mathbf{r}_e;\mathbf{r}_p)$.

The electric-field approach introduced by Harbola and Sahni[27] for determining electron-electron correlations and exchange at a metal surface seems to be promising for the description of electron-positron interactions. I would like to suggest the adaptation of the formalism of Ref. 27 to the positron-surface problem. The correlation potential acting on the positron at $\mathbf{r}_p$ may be interpreted as the work done in moving a positron from infinity up to its final position against the electric field $\mathcal{E}_{\mathrm{corr}}$ coming from the electronic screening cloud:

$$V_{\mathrm{corr}}(\mathbf{r}_p)=-\int_{-\infty}^{\mathbf{r}_p}\mathcal{E}_{\mathrm{corr}}d\mathbf{l} \ , \tag{7a}$$

where the electric field felt by a positron at $\mathbf{r}_p$ is given by

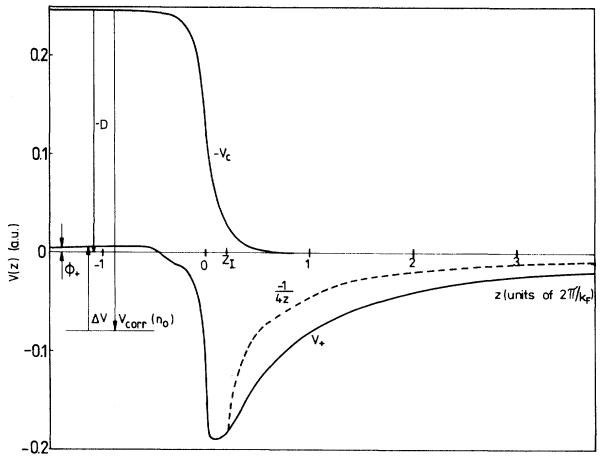

FIG. 1. Effective potential acting on the positron at the surface, $V_+(z_p)=-V_C(z_p)+V_{\mathrm{corr}}(z_p)+\Delta V\Theta(-z_p)$, and its Hartree part $-V_C(z_p)$. $\phi_+=-0.19$ eV is a positron work function, $\Delta V=2.34$ eV is the height of the potential step, z_I is the position of the image plane, and $V_{\mathrm{corr}}(n_0)=-a^3(n_0)/4$ is a correlation potential in the bulk. The classical image potential is denoted by a dashed lined.

the Coulomb law

$$\mathcal{E}_{\rm corr}(\mathbf{r}_p)=\int d\mathbf{r}_e \Delta\rho(\mathbf{r}_e;\mathbf{r}_p)\frac{(\mathbf{r}_e-\mathbf{r}_p)}{|\mathbf{r}_e-\mathbf{r}_p|^3}\ . \tag{7b}$$

In the calculations of the present work, the approach based on the Feynman theorem[18,24,26] is used. The electron-positron interaction, scaled by the interaction parameter Q, is included adiabatically; i.e., Q is increased from zero (no interaction) to unity (full interaction corresponding to the actual state of the system). Since the electron-positron correlations are mainly due to the Coulomb forces, the interaction parameter Q can be considered as the charge of a light particle embedded in the many-electron system.[26] This particle causes the change in the background charge density $n_{\rm el}(\mathbf{r})$, and an electronic screening cloud $\Delta\rho(\mathbf{r}_e;\mathbf{r}_p,Q)$ arises. The distribution $\Delta\rho(\mathbf{r}_e;\mathbf{r}_p,Q)$ is obviously an increasing function of Q. For $Q=1$ (actual interaction) one has $\Delta\rho(\mathbf{r}_e;\mathbf{r}_p,Q=1)=\Delta\rho(\mathbf{r}_e;\mathbf{r}_p)$ and for $Q=0$ (no interaction) $\Delta\rho(\mathbf{r}_e;\mathbf{r}_p,Q=0)=0$. In terms of the displaced charge-correlation function of the one-positron many-electron system,

$$g(\mathbf{r}_e,\mathbf{r}_p,n_{\rm el},Q)=1+\Delta\rho(\mathbf{r}_e;\mathbf{r}_p,Q)/n_{\rm el}(\mathbf{r}_e)\ , \tag{8}$$

the charge-neutrality condition has the form

$$\int d\mathbf{r}_e n_{\rm el}(\mathbf{r}_e)[g(\mathbf{r}_e,\mathbf{r}_p,n_{\rm el},Q)-1] = \int d\mathbf{r}_e \Delta\rho(\mathbf{r}_e;\mathbf{r}_p,Q)=Q\ , \tag{9}$$

for any $\mathbf{r}_p$ and Q.[26]

It should be noted here that the present understanding of the interaction parameter Q differs from its interpretation by Jensen and Walker,[18] who included the parameter Q into the electron-coupling constant as a factor. The authors of Ref. 18 employed, following Gunnarson, Johnson, and Lundqvist,[24] the normalization condition

$$\int_0^1 dQ \int d\mathbf{r}_e n_{\rm el}(\mathbf{r}_e)[g(\mathbf{r}_e,\mathbf{r}_p,n_{\rm el},Q)-1] = \int_0^1 dQ \int d\mathbf{r}_e \Delta\rho(\mathbf{r}_e;\mathbf{r}_p,Q)=1\ , \tag{10a}$$

for any $\mathbf{r}_p$, where the parameter Q scaled the electronic screening length. At the same time, according to Eq. (2c), the condition

$$\int d\mathbf{r}_e n_{\rm el}(\mathbf{r}_e)[g(\mathbf{r}_e,\mathbf{r}_p,n_{\rm el},Q=1)-1] = \int d\mathbf{r}_e \Delta\rho(\mathbf{r}_e;\mathbf{r}_p)=1 \tag{10b}$$

had to be fulfilled. This problem will be also discussed in Sec. II B.

The correlation potential acting on the positron located at $\mathbf{r}_p$ can be expressed according to the Feynman theorem[18,24,26] as

$$V_{\rm corr}(\mathbf{r}_p)=-\int_0^1 dQ \int d\mathbf{r}_e n_{\rm el}(\mathbf{r}_e) \times[g(\mathbf{r}_e,\mathbf{r}_p,n_{\rm el},Q)-1]/|\mathbf{r}_e-\mathbf{r}_p| =-\int_0^1 dQ \int d\mathbf{r}_e \Delta\rho(\mathbf{r}_e;\mathbf{r}_p,Q)/|\mathbf{r}_e-\mathbf{r}_p|\ . \tag{11}$$

Equation (7) or (11) gives the relation between the change in the electron-density distribution $\Delta\rho(\mathbf{r}_e;\mathbf{r}_p)$ and the correlation part of the effective potential acting on the positron, $V_{\rm corr}(\mathbf{r}_p)$, which we should be aware of in the calculation of positron-annihilation characteristics (at the surface as well as in the bulk[20]). From Eqs. (7) and (11) it clearly follows that if $\Delta\rho(\mathbf{r}_e;\mathbf{r}_p)=\Delta\rho(|\mathbf{r}_e-\mathbf{r}_p|)$ (i.e., it is independent of positron position $\mathbf{r}_p$), then $V_{\rm corr}(\mathbf{r}_p)=V_0$ and the effective potential acting on a positron differs from the Hartree potential $-V_C(\mathbf{r}_p)$ only by the constant value V_0. In this case the positron wave function is the eigenfunction of the Schrödinger equation[19]

$$[-\tfrac{1}{2}\nabla_p^2-V_C(\mathbf{r}_p)]\psi_+^0(\mathbf{r}_p)=E_+^0\psi_+^0(\mathbf{r}_p)\ . \tag{12}$$

The relation between the screening charge distribution and correlation potential is reversible; i.e., the effective positron potential $V_+(\mathbf{r}_p)$ may be replaced in Eq. (6a) by its Coulomb part $-V_C(\mathbf{r}_p)$ [Eq. (12)] only if $\Delta\rho(\mathbf{r}_e;\mathbf{r}_p)=\Delta\rho(|\mathbf{r}_e-\mathbf{r}_p|)$. This obviously occurs when the positron interacts with a homogeneous electron system of a constant background electron density $n_{\rm el}(\mathbf{r})=n_0$. In real metals, however, the equivalence between $\Delta\rho(\mathbf{r}_e;\mathbf{r}_p)$ and $V_{\rm corr}(\mathbf{r}_p)$ should be taken into account[20] when the positron-annihilation characteristics for a positron in a surface state or in the bulk are calculated, according to Eqs. (3b) and (3a) and (4) or (5).

Let us discuss the applicability of the independent-particle model (IPM) to the surface problem from the above point of view. Within the IPM the electron-positron correlations are neglected. If we want to apply the IPM strictly [i.e., to assume $F(\mathbf{r})=f(\mathbf{r},i)=1$], we should neglect $V_{\rm corr}(\mathbf{r})$. The pair wave functions $\psi_i^{ep}(\mathbf{r}_e,\mathbf{r}_p)$ in the ACAR and lifetime formulas (3a) and (3b), respectively, are replaced by the products $\psi_i^0(\mathbf{r}_e)\psi_+^0(\mathbf{r}_p)$, where the positron wave function ψ_+^0 is an eigenfunction of the Schrödinger equation (12) [instead of (6b)]. This leads to the well-known formulas for the IPM annihilation characteristics:

$$\rho^{\rm IPM}(\mathbf{p})=\sum_{i_{\rm occ}}\left|\int e^{-i\mathbf{p}\cdot\mathbf{r}}\psi_i^0(\mathbf{r})\psi_+^0(\mathbf{r})d\mathbf{r}\right|^2 \tag{13a}$$

and

$$\lambda^{\rm IPM}=\pi r_0^2 c\int|\psi_+^0(\mathbf{r})|^2 n_{\rm el}(\mathbf{r})d\mathbf{r}\ . \tag{13b}$$

It should be noted here that in the bulk the ACAR spectra are reproduced within the IPM reasonably well, at least for valence electrons in the simple metals and in the low-momentum region (the discrepancies between the IPM and experiment are pronounced for momenta approaching the Fermi momentum[21,22] and higher as well as in d-electron metals[19,28] or at ionic cores[20,28(b)]). It is not so with the positron lifetime, which, within the IPM, is considerably overestimated [Eq. (13b)]. At the metal surface, however, the applicability of the IPM is limited. As is seen in Fig. 1, the potential $-V_C(\mathbf{r}_p)$ has a strongly repulsive character, and if $V_{\rm corr}(\mathbf{r}_p)$ were constant (or equal to zero), the unscreened surface positron in its ground state E_+^0 [Eq. (12)] would be repelled to the vacuum. The normalized positron wave function ψ_+^0 would

be constant far in the vacuum and exponentially vanish into the metal because of the positron tunneling through the dipole barrier of height $-V_C(-\infty)-[-V_C(\infty)]$. This means that within this model no positron surface state would be formed. The positron wave function ψ_+^0 would be smeared in the vacuum, while electrons are confined to the metal. Thus the overlaps of $\psi_+^0(\mathbf{r})$ and $\psi_i^0(\mathbf{r})$ [cf. Eq. (13a)] would be very small, and therefore the information about the electron distributions at the surface extractable from the IPM ACAR spectrum would be fairly poor. For this reason in several theoretical works[11,12] calculations of the surface ACAR spectra were performed within a modified model, called in the present work the quasi-IPM in order to distinguish it from the "true" IPM. Within the quasi-IPM the change in the density of electronic states on the positron is neglected as within the IPM [i.e., it is assumed that $\psi_i(\mathbf{r}_p;\mathbf{r}_p)=\psi_i^0(\mathbf{r}_p)$], but the positron at the surface is influenced by the electron-positron correlation potential $V_{\rm corr}(\mathbf{r}_p)\neq$const.

It should be stressed here that the quasi-IPM is well justified for positron positions far in the vacuum. In this case the electronic screening cloud would be detached from the positron[17] [i.e., $\Delta\rho(\mathbf{r}_p;\mathbf{r}_p)=0$] and localized at the image plane located at $z=z_I$ (see dotted line in Fig. 2 and solid line in Fig. 3). The image charge[25] should produce the electron-positron correlation potential in the classical image form $V_{\rm corr}(\mathbf{r}_p)=-0.25/(z_p-z_I)$, according to Eqs. (7) and (11). However, the contribution of this region to positron-annihilation characteristics (3a) and (3b) [(13a) and (13b)] is negligible because both the electron and positron densities decrease rapidly as the positron escapes to the vacuum.

In the bulk and near-surface region, which give the main contribution to the partial and total annihilation rates, the quasi-IPM is internally inconsistent. Since this particular point could raise some controversies, I found it necessary to add some comments. As is illustrated in Fig. 2 (dashed, solid, and dot-dashed lines), for positron positions in the bulk and between the surface and image planes (i.e., for $z_p\leq z_I$), the screening charge density $\Delta\rho(\mathbf{r}_e;\mathbf{r}_p)$ achieves its maximum either just on the positron, i.e, for $\mathbf{r}_e=\mathbf{r}_p$, or in its immediate vicinity. Thus, for $z_p<z_I$, the assumption $\Delta\rho(\mathbf{r}_p;\mathbf{r}_p)=0$ implies that $\Delta\rho(\mathbf{r}_e;\mathbf{r}_p)\cong 0$ for any $\mathbf{r}_e$, and therefore $V_{\rm corr}(\mathbf{r}_p)=0$, according to Eqs. (7) and (11), but in disagreement with the quasi-IPM assumption $V_{\rm corr}(\mathbf{r}_p)\neq$const. For this reason the quasi-IPM must be treated with a great deal of caution in the region $z_p\leq z_I$. On the other hand, as can be seen in Fig. 1, the positions $z\leq z_I$ occupy an appreciable part of the positron potential well, where the positron is found. Because of this deficiency, the quasi-IPM ACAR spectra[11,12] should not be compared directly with the experimental data. The momentum density $\rho(\mathbf{p})$ [Eq. (3a) or (5)], whose 2D projections are measured experimentally, differs from the quasi-IPM distribution $\rho_q^{\rm IPM}(\mathbf{p})$ by a momentum-dependent enhancement factor $\epsilon_{\rm MD}(\mathbf{p})$, defined as

$$\epsilon_{\rm MD}(p)=\rho(\mathbf{p})/\rho_q^{\rm IPM}(\mathbf{p}) .$$

Here a remark is needed. The positron is a strongly interacting probe, and hence it measures properties of excited (N-electron+positron) states. In practice, however, we are interested in the ground (N-electron) state of the system. In the calculations of $\rho(\mathbf{p})$, which corresponds to experimental ACAR spectra, the electron-positron correlations are included both to the electron and positron wave functions, according to Eqs. (2a) and (7) or (11). The quasi-IPM, despite its deficiencies, reflects the positron and *unperturbed* electron distributions at the surface [cf. Eq. (13a)], i.e., the quantities just under study. Since quasi-IPM ACAR spectra must not be related directly to experimental ones, in the interpretation of slow-positron experimental data the knowledge of enhancement factors $\epsilon_{\rm MD}(\mathbf{p})$ is needed.

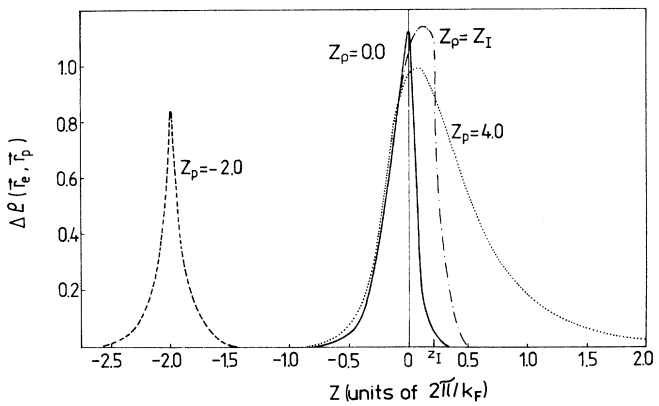

FIG. 2. Cross sections of the screening charge distribution $\Delta\rho(0,z_e;z_p)$ for various positron positions z_p: in the bulk (dashed line, $\Delta\rho$ enlarged 10 times), at the surface plane (solid line, enlargement 20), at the image plane z_I (dot-dashed line, enlargement 50), and well outside the metal (dotted line, enlargement 100).

B. Electron-positron correlations at the surface

In order to determine correctly the positron-annihilation characteristics at the surface, the screening charge distribution $\Delta\rho(\mathbf{r}_e;\mathbf{r}_p)$ should be known [cf. Eqs. (3b) and (5) as well as Eqs. (7) and (11) for a positron]. For positron positions well inside the metal, the screening charge distribution may be considered as spherically symmetric (if the lattice effects are neglected). As a positron approaches the surface from inside the metal, the polarization cloud flattens along a surface[17,18] and becomes detached, forming a classical image charge for a positron located far in the vacuum (this gives rise to an image form of the correlation potential).[17,25]

Preliminary calculations of the electronic charge distribution screening a positron moving from the metal to vacuum were performed by Inglesfield and Stott[17] within the random-phase approximation (RPA) and in the infinite-barrier model of a metal surface. Although the formalism of Ref. 17 led to quantitatively correct results for the shape of the polarization cloud and positron-correlation energy, nevertheless, these calculations cannot be considered as definitive. As is well known, the

RPA does not give a satisfactory account of electron-positron correlations in the range of metallic and low densities (it is valid for high densities only[19–22]). Also, the dipole barrier at the real-metal surface is of finite height.

Electron-positron correlations, applied in the present work to calculating of positron-annihilation characteristics at metal surface, are determined within the weighted-density approximation (WDA).[18,24] The WDA is in principle an adaptation of the LDA to strongly inhomogeneous systems. It should be stressed here that although the WDA allows us to go beyond the RPA and is based on more realistic electron-density profiles at the surface than those resulting from the infinite-barrier model,[17] nevertheless, the calculations of the screening charge distributions $\Delta\rho(\mathbf{r}_e;\mathbf{r}_p)$ performed within the WDA are not self-consistent in the sense of Hohenberg-Kohn-Sham theory.[23(a),23(b)]

Within the WDA the displaced-charge correlation function of the system is approximated by

$$g(\mathbf{r}_e,\mathbf{r}_p,n_{\rm el},Q)_{\rm WDA}=g^h(|\mathbf{r}_e-\mathbf{r}_p|,n^*(\mathbf{r}_p),Q)\ ,$$

where $g^h(r,n^*,Q)$ is the correlation function in an electron gas of density n^*. The corresponding screening charge distributions and positron-correlation potential are equal to

$$\Delta\rho(\mathbf{r}_e;\mathbf{r}_p,Q)_{\rm WDA}=n_{\rm el}(\mathbf{r}_e)[g^h(|\mathbf{r}_e-\mathbf{r}_p|,n^*(\mathbf{r}_p),Q)-1] \tag{14a}$$

and

$$V_{\rm corr}(\mathbf{r}_p)_{\rm WDA}=-\int_0^1 dQ\int d\mathbf{r}_e n_{\rm el}(\mathbf{r}_e)[g^h(|r_e-r_p|,n^*(\mathbf{r}_p),Q)-1]\ , \tag{14b}$$

according to Eqs. (8) and (11), respectively. The values of the effective electron density $n^*(\mathbf{r}_p)$ are determined for any $\mathbf{r}_p$ from charge-neutrality conditions (9), which is treated as an equation for $n^*(\mathbf{r}_p)$.

For practical applications of the WDA to the positron surface problem, first of all the form of the displaced-charge correlation function in jellium must be known. In an electron gas of density n^*, this function may be approximated by an exponential form.[29,26,21,18] Assuming an exponential distribution of the electronic cloud screening a heavy-particle-charged Q,[30] the screening length remains unchanged when Q increases, unlike the density of the screening charge on the particle, which is proportional to Q. Thus the correlation function $g^h(r,n^*,Q)$ may be assumed in the form

$$g^h(|\mathbf{r}_e-\mathbf{r}_p|,n^*,Q)=1+Q\frac{a^3(n^*)}{8\pi n^*}e^{-a(n^*)|\mathbf{r}_e-\mathbf{r}_p|}\ , \tag{15a}$$

where the form of $g^h(0,n^*,1)$, enabling us to calculate $a(n^*)$, was parametrized in Refs. 23(d) and 23(e) as a function of n^*. For low and metallic electron densities, occurring at the surface, the results of Refs. 23(d) and 23(e) are in fairly good agreement with the more convenient, in practical applications Brandt-Reinheimer formula,[31] which leads to a simple density-dependent form of $a(n^*)$:[26,18]

$$a^3(n^*)=1+40\pi n^*/3\ , \tag{15b}$$

employed in the calculations of the present work.

For an electron gas of constant electron density $n_{\rm el}(\mathbf{r})=n^*$, the correlation functions given by Eq. (15a) clearly satisfy the charge-neutrality conditions (9) and the correct values of total annihilation rates in jellium,[31] $\lambda(n^*)$, are reproduced for low and metallic densities. The corresponding correlation energies obtained according to Eq. (14b), equal to $V_{\rm corr}(n^*)=-a(n^*)/4$, are in good agreement with their n^* dependence[23(d)] in the range of low and metallic electron densities. The form (15a) of correlation function in jellium, assumed in the present work, differs from the one used in Ref. 18, where the parameter Q scaled the electron screening length $Qa(n^*)$ and the charge-neutrality conditions (10a) and (10b) were employed. Although the annihilation parameters in jellium, $V_{\rm corr}(n^*)$ and $\lambda(n^*)$, resulting from the present approach and the one of Ref. 18, are exactly the same, nevertheless, for an inhomogeneous electron system (metal surface), the correlation function in the form (15a) enables us to avoid the deficiency contained in Ref. 18. The charge-neutrality conditions (10a) and (10b) used in Ref. 18 determined *two different* effective WDA electron densities for a positron located outside a metal, $n_1^*(\mathbf{r}_p)$ and $n_2^*(\mathbf{r}_p)$, respectively. Both these densities were applied simultaneously in the *one* lifetime formula (3b). The density $n_1^*(\mathbf{r}_p)$ was used for determining the correlation potential in the positron Scrödinger equation, while the enhancement of the electron density on the positron depended on $n_2^*(\mathbf{r}_p)$. In contrast to Ref. 18, the present approach leads to *one* effective electron density $n^*(\mathbf{r}_p)$, satisfying the charge-neutrality conditions (9) for any $Q\in[0,1]$.

The correlation potential obtained within the WDA according to Eqs. (14b) and (15b) is given by the expression

$$V_{\rm corr}(\mathbf{r}_p)=-\frac{a^3[n^*(\mathbf{r}_p)]}{8\pi n^*(\mathbf{r}_p)}\times\int d\mathbf{r}_e e^{-a[n^*(\mathbf{r}_p)]|\mathbf{r}_e-\mathbf{r}_p|}\times n_{\rm el}(\mathbf{r}_e)/|\mathbf{r}_e-\mathbf{r}_p|\ . \tag{16}$$

The screening charge density calculated according to Eqs. (14a) and (15b),

$$\Delta\rho(\mathbf{r};\mathbf{r})=n_{\rm el}(\mathbf{r})\frac{a^3[n^*(\mathbf{r})]}{8\pi n^*(\mathbf{r})}$$
$$=n_{\rm el}(\mathbf{r})\left[\frac{5}{3}+\frac{1}{8\pi n^*(\mathbf{r})}\right], \quad (17)$$

leads to the formula, for a total annihilation rate,

$$\lambda=\pi r_0^2 c\int d\mathbf{r}|\psi_+(\mathbf{r})|^2 n_{\rm el}(\mathbf{r})\left[1+\frac{a^3[n^*(\mathbf{r})]}{8\pi n^*(\mathbf{r})}\right]$$
$$=\lambda^{\rm IPM}+\frac{r_0^2 c}{8}\int d\mathbf{r}|\psi_+(\mathbf{r})|^2 a^3[n^*(\mathbf{r})]\frac{n_{\rm el}(\mathbf{r})}{n^*(\mathbf{r})}\ . \quad (18)$$

Within the WDA the displaced-charge correlation function of the system, $g(\mathbf{r}_e,\mathbf{r}_p,n_{\rm el},Q)$, is replaced for any $\mathbf{r}_p$ by its analog in an electron gas of the effective density $n^*(\mathbf{r}_p)$, $g^h(|\mathbf{r}_e-\mathbf{r}_p|,n^*(\mathbf{r}_p),Q)$. Since, according to Eq. (4), $g(\mathbf{r}_p,\mathbf{r}_p,n_{\rm el},Q=1)$ is a weighted average of individual enhancement functions $f(\mathbf{r}_p,i)$, the functions $f(\mathbf{r}_p,i)$ employed in the ACAR formula (3a) may be also replaced within the WDA by their analog in an electron gas of density $n^*(\mathbf{r}_p)$, $\epsilon^B(\sqrt{E_i/E_F},n^*(\mathbf{r}_p))$.[15,19,20,28(a),28(b)] Here $\epsilon^B(p,n^*)$ are electron-positron enhancement factors obtained within the model of jellium for various electron densities n^*,[21,22] and E_F is a Fermi energy. Since $\epsilon^B(p,n^*)$ as functions of n^* behave as $(n^*)^{-1}$, while, as functions of p, increase at most 50%,[21,22,23(e)] the position dependence of $f(\mathbf{r},i)$ is much more pronounced at the surface and in the vacuum (where a positron is found) than their state dependence. For this reason $f(\mathbf{r},i)$ may be approximated in the ACAR formula (3a) by their average over i, given by Eq. (4). The latter leads to expression (5) for momentum density $\rho(\mathbf{p})$, used in the present work. It should be noted here that the use of the SS ACAR formula (5) instead of (3a) is not only a numerical simplification which does not change the results (as checked numerically in the case of an ideal Al surface). It is an essential advantage in comparison with (3a), as it allows one to avoid determining individual electron-positron correlations separately, at the same time conserving the shape of the ACAR spectra. This problem is discussed also in Ref. 16.

For the correlation function in the form (15b), Eqs. (17) and (5) lead to the WDA ACAR formula

$$\rho(\mathbf{p})=\sum_{i_{\rm occ}}\left|\int d\mathbf{r}\,e^{-i\mathbf{p}\cdot\mathbf{r}}\psi_+(\mathbf{r})\psi_i^0(\mathbf{r})\times\{1+a^3[n^*(\mathbf{r})]/[8\pi n^*(\mathbf{r})]\}^{1/2}\right|^2 . \quad (19)$$

III. CALCULATIONS AND RESULTS

In this section the annihilation characteristics from an ideal Al surface are presented. Calculations were performed within the jellium model, where the ions are thought of as forming a constant positive background charge within the metal, $n_{\rm ion}(z)=n_0\Theta(-z)$. Here $n_0=3/(4\pi r_s^3)$ is the bulk conduction-electron density, r_s is a Wigner-Seitz radius [for Al, $r_s=2.07$ (Ref. 30)], $\Theta(z)$ is the Heaviside step function, and the coordinate z is perpendicular to the surface. The positron and unperturbed electron wave functions at the surface are assumed in the form

$$\psi_+(\mathbf{r})=S^{-1/2}\psi_+(z) \quad (20a)$$

and

$$\psi_{\mathbf{k}}^0(\mathbf{r})=\frac{1}{\sqrt{S}}e^{i(k_x x+k_y y)}\psi_{k_z}(z)\ , \quad (20b)$$

respectively, where $\mathbf{r}=(x,y,z)$ and S is the area of the surface plane. The functions $\psi_{k_z}(z)$ obey the set of Schrödinger equations [cf. Eqs. (6a) and (20a)]

$$\left[-\frac{d^2}{dz^2}+2V_{\rm eff}(z)\right]\psi_{k_z}(z)=(k_z^2-k_F^2)\psi_{k_z}(z)\ , \quad (21a)$$

with boundary conditions $\psi_{k_z}(\infty)=0$ and $\psi_{k_z}(-\infty)=\sin[k_z+\delta(k_z)]$, where the phase shifts are continuous and $\delta(0)=0$. The Coulomb part of the effective electron potential (cf. Sec. II A) satisfies the Poisson equation

$$\frac{d^2}{dz^2}V_C(z)=-4\pi[n_{\rm el}(z)-n_{\rm ion}(z)]\ , \quad (21b)$$

where the background electron charge density $n_{\rm el}(z)$ is, according to Eq. (2b), equal to

$$n_{\rm el}(z)=\frac{1}{\pi^2}\int_0^{k_F}(k_F^2-k_z^2)[\psi_{k_z}(z)]^2 dk_z\ . \quad (21c)$$

k_F in Eqs. (21a) and (21c) denotes the Fermi momentum in the bulk. The electron-electron exchange and correlations were treated in a local way, and the Wigner's form[32] of $V_{\rm xc}(n_{\rm el}(z))$ was used. Equations (21a)–(21c) were solved self-consistently[15] within an iterative scheme proposed by Manninen *et al.*[33(a)] and adapted to finite space by Monnier and Perdew.[33(b)] The details of the calculations and results are given in Ref. 15. The electron-density profile $n_{\rm el}(z)$ as well as the potentials $V_C(z)$ and $V_{\rm eff}(z)$ are presented in Figs. 1 and 2 of Ref. 15, respectively.

Here a remark should be made. As is well known, real metals differ from an electron gas. For simple metals, however, characterized by nearly parabolic valence bands, the jellium model describes electron wave functions in the interstitial region reasonably well. In particular, conduction electrons in bulk aluminum have a nearly free nature. As was pointed out by Monnier and Perdew,[33(b)] the Al(100) face is also jelliumlike. The projected energy-band structure for each of three low-index surfaces of Al was determined by Chen *et al.*[4] The bottom of the bands are parabolic, while substantial gaps appear below and above the Fermi energy. The energy gaps near the Fermi level have a crucial effect on the positronium-emission spectroscopy results,[4] since the electron energy distribution near the Fermi energy is decisive in the theoretical Ps momentum density.[1(a),4] In contrast to the Ps component, the SS ACAR spectra are dependent mainly on the shape of the electron wave func-

tions (cf. discussion in Sec. II), while the electron energies are considered in the SS ACAR formula (5) in the average [cf. Sec. II B and, in particular, formulas (4) and (5)]. The nearly free electron nature of Al conduction bands allows one to substantiate the approximation of the electron wave functions at the surface in the form (20a), at least for the Al(100) face. The fact that the lattice effects are neglected parallel to the surface is, however, reflected in $N(p_x)$ in the high-momentum region [the density $N(p_x)$ obtained within the jellium model of the metal surface vanishes for momenta $p_x \geq k_F$].

The distribution of electronic charge screening a positron located at $\mathbf{r}_p=(x_p,y_p,z_p)$, $\Delta\rho(\mathbf{r}_e;\mathbf{r}_p)$, was modeled within the WDA, according to Eqs. (14a), (15a), and (15b). Within the jellium model $\Delta\rho(\mathbf{r}_e;\mathbf{r}_p)$ may be written in the form

$$\Delta\rho(\mathbf{r}_e;\mathbf{r}_p)=\Delta\rho(R,z_e;z_p)\ ,$$

where

$$R=[(x_e-x_p)^2+(y_e-y_p)^2]^{1/2}\ ,$$

$$n^*(\mathbf{r}_p)=n^*(z_p),\quad \text{and}\quad V_{\rm corr}(\mathbf{r}_p)=V_{\rm corr}(z_p)\ .$$

The effective WDA electron density $n^*(z_p)$ was obtained for any z_p according to charge-neutrality conditions (9). For positron positions z_p well inside the metal, the values of the effective density $n^*(z_p)$ coincide with $n_{\rm el}(z_p)$. When the positron is in the vacuum ($z_p\to\infty$), $n_{\rm el}(z_p)/n^*(z_p)\to 0$. For $z_p\to\infty$, however, $n^*(z_p)\to 0$ as well.

The cross sections of the resulting screening charge density $\Delta\rho(0,z_e;z_p)$ for various positron positions z_p are shown in Fig. 2. The screening cloud, which is spherically symmetric in the bulk (dashed line in Fig. 2), deforms as the positron approaches the surface (solid line in Fig. 2) and is left behind at the image plane located at $z_I=1.76$ a.u. for positron positions far in the vacuum (dotted line in Fig. 2). This is also illustrated in Fig. 3, where the positions of the center of mass of the screening cloud, defined as[25]

$$z_0(z_p)=\int d^2\mathbf{R}\int_{-\infty}^{\infty}dz_e z_e\Delta\rho(R,z_e;z_p)\Big/\int d^2\mathbf{R}\int_{-\infty}^{\infty}dz_e\Delta\rho(R,z_e;z_p)\ , \tag{22}$$

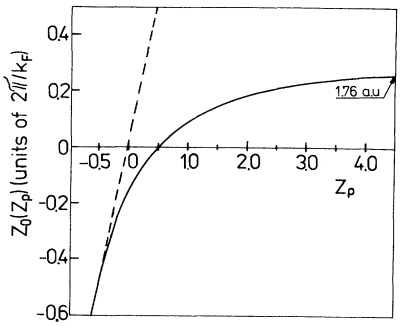

FIG. 3. Positions of the center of mass of the screening charge distribution [Eq. (22)] as a function of a positron position (solid line) compared with the function $z_1(z_p)=z_p$ (dashed line).

are presented by a solid line for various positron position z_p. The function $z_1(z_p)=z_p$ is shown for comparison (dashed line). For positron positions well inside the metal, $z_0(z_p)=z_p$; i.e., the center of mass of the polarization cloud is on the positron. As the positron leaves the metal, the center of mass becomes detached (see deviation between solid and dashed curves in Fig. 3), and for the positron located far in the vacuum, ($z_p\to\infty$) $z_0(z_p)\to z_I=1.76$ a.u. [the relation between the position of the image plane z_I and the limit value of $z_0(z_p)$ for $z_p\to\infty$ is discussed in Ref. 25].

The positron-correlation potential $V_{\rm corr}(z_p)$ was obtained according to Eq. (16). The asymptotic behavior of $V_{\rm corr}(z_p)\to -1/[2(z_p-z_I)]$ for $z_p\to\infty$ is observed (see solid line in Fig. 1). For comparison the classical image potential $V_{\rm im}(z_p)=-1/(4z_p)$ is given in Fig. 1 (dashed line). The deviation of $V_{\rm corr}(z_p)$ from the image form by a factor $\frac{1}{2}$ may be attributed to the fact that the calculations of electron-positron correlations, performed within the WDA, are not self-consistent in the sense of HKS theory, as was pointed out in Sec. II B. The screening charge distribution on the image plane,

$$\Delta\rho(R,z_I;z_p)=n_{\rm el}(z_I)\frac{a^3[n^*(z_p)]}{8\pi n^*(z_p)}\times e^{-a[n^*(z_p)][R^2+(z_I-z_p)^2]^{1/2}}\ ,$$

determined according to Eq. (15a), never achieves the image form obtained by Lang[25] for a heavy particle located far away from the jellium metal surface,

$$\Delta\rho_{\rm im}(R,z_I;z_p)=\frac{(z_p-z_I)}{2\pi[R^2+(z_p-z_I)^2]^{3/2}}\ .$$

The screening charge density $\Delta\rho(R,z_I;z_p)$ in the form (15a) decreases exponentially as a function of R for any positron position z_p, while $\Delta\rho_{\rm im}(R,z_I;z_p)$ behaves as R^{-3} for $z_p\to\infty$. Moreover, as follows clearly from Eq. (17), although the electron density on the positron, $\Delta\rho(0,z_p;z_p)$, tends to zero for positron positions well outside the metal, nevertheless, the screening cloud is never completely detached from the positron, since, for $z_p\to\infty$, $\Delta\rho(0,z_p;z_p)$ converges to zero weaker than $n_{\rm el}(z_p)$, and in consequence $g(\mathbf{r}_p,\mathbf{r}_p,n_{\rm el},Q=1)$ differs from unity for large values of z_p. Thus electron-positron correlations for the positron located far in the vacuum are overestimated within the WDA. Since the WDA gives a correct account of the average correlation energy,[24] the electron-positron correlations in the immediate vicinity of the surface are likely to be slightly underestimated.

The effective positron potential $V_+(z_p)$ is the sum of electron Hartree (with opposite sign) and electron-positron correlation potentials. The positron work function $\phi_+=V_+(\infty)-\mu_p$ is the difference between the

effective positron potential in vacuum and the bulk positron chemical potential μ_p, which, within the jellium model, is equal to $\mu_p^{\text{jell}} = -V_C(-\infty) + V_{\text{corr}}(-\infty)$. For $z_p \to \infty$ we have $V_{\text{corr}}(\infty) \to 0$ and hence the corresponding positron work function in jellium $\phi_+^{\text{jell}} = -D - V_{\text{corr}}(-\infty)$, where $D = V_C(\infty) - V_C(-\infty)$ is the height of the surface-dipole-layer potential. However, the model of jellium, used in the calculations of the present work, neglects the interaction of electrons and the positron with the ionic lattice.

In real metals the surface-dipole-layer potential may be considerably different from the value calculated in the jellium model. This is because the potential of the lattice of ions, experienced by electrons, is considerably more attractive than the electrostatic potential of the jellium positive background, and the electron Fermi level, or the internal chemical potential μ_e, becomes more negative than for jellium.[34] Lang and Kohn,[35] Monnier and Perdew,[33(b)] and Perdew, Tran, and Smith[34(c)] considered the difference between the potentials of the semi-infinite lattice of ions and the electrostatic potential of the semi-infinite uniform positive background. The "difference potential" $\delta v_{\text{WS}}(\mathbf{r})$ in the neutral Wigner-Seitz cell was defined in Refs. 33(b) and 34(c) as the sum of the pseudopotential in this cell and the electrostatic potential of the uniform electronic density contained within it, with the convention that $\delta v_{\text{WS}}(\mathbf{r})$ vanishes far outside it. The average of $\delta v_{\text{WS}}(\mathbf{r})$ over a Wigner-Seitz sphere, $\langle \delta v_{\text{WS}} \rangle$, was found to be a considerable fraction of both the free-electron Fermi energy and one-electron potential barrier of the jellium surface. The change in D, however, almost cancels the change in μ_e, leaving the electron work function relatively insensitive to the strength of the electron-ion interaction. The authors of Refs. 33(b) and 34(c) proposed to approximate the potential $\delta v_{\text{WS}}(\mathbf{r})$ by a step function $\langle \delta v_{\text{WS}} \rangle \Theta(-z)$, where the structureless step height $\langle \delta v_{\text{WS}} \rangle$ for Al was estimated as -2.4 eV [Ref. 33(b)] or -2.49 eV [Ref. 34(c)].

In contrast to electrons, the positron is strongly repelled from the ions, and in some cases the lowest positron state lies several electronvolts above the electrostatic potential in the interstitial region, and the positron chemical potential μ_p is more positive than for jellium.[34(a),36] One can mimic this additional dipolar effect by subtracting from the positron potential the electron difference potential $\delta v_{\text{WS}}(\mathbf{r})$ or its approximation $\langle \delta v_{\text{WS}} \rangle \Theta(-z)$.[33(b),34(c)] In the present electron model, this correction leads to the positron work function $\phi_+ = -0.25$ eV for $\langle \delta v_{\text{WS}} \rangle = -2.4$ eV [Ref. 33(b)] and $\phi_+ = -0.34$ eV for $\langle \delta v_{\text{WS}} \rangle = -2.49$ eV.[34(c)] In the present work the step height $\Delta V = -2.34$ eV was adjusted in order to reproduce the experimental value of a positron work function for an Al(100) face, equal $\phi_+ = -0.19$ eV.[1(a),1(d)] In Fig. 1 the effective positron potential $V_+(z)$ and its Coulomb part $-V_C(z)$ as well as the potential step ΔV are presented. It should be noted here that ΔV is a fitting parameter, necessary in order to switch from the jellium model to a real-metal surface. This method is used in the majority of calculations of positron wave functions at the metal surface (cf., e.g., Refs. 11–13, 15, 18, 36, and 37), and we would be able to avoid imposing the step potential $\Delta V \Theta(-z)$ only if fully self-consistent calculations of the electron Hartree potential V_C at real-metal surfaces were performed.

The positron wave function $\psi_+(z_p)$ was obtained according to Eq. (6b). The resulting value of the positron binding energy E_B relative to the bulk, equal to -3.06 eV, is in good agreement with slow-positron experimental data for Al(100) face, $E_B = -3.05$ eV [Ref. 1(a)] or -2.8 eV.[1(d)] It should be noted here that the eigenvalues of Eq. (6b) (and, henceforth, positron binding energy E_B) are dependent not only on the depth of the potential well, but also on the shape of correlation potential in vacuum. When the image potential was imposed in vacuum instead of V_{corr} (see Fig. 1), the resulting value of binding energy changed to $E_B = -2.9$ eV.

The total annihilation rate λ was obtained within the WDA according to Eq. (18). The value of the positron lifetime, $\tau = 593$ psec, is in good agreement with slow-positron measurements for the Al(100) face, $\tau_{\text{exp}} = 580$ psec.[10] Comparison of theoretical annihilation rates with experimental ones allows one to deduce that the jellium model of the Al(100) surface is a reasonable approximation when the positron surface state is investigated. The long positron SS lifetime should not be attributed to trapping of a positron at the surface defects, as claimed by Brown *et al.*,[12] and a proper treatment of electron-positron correlations at the surface seems to be much more important than lattice effects. My feeling is that the statement of Jensen and Walker,[18] "... an asymptotic limit [of $V_{\text{corr}}(z_p)$] is unlikely to seriously affect the properties of the positron surface state...," is not quite exact. When far in the vacuum the image potential was imposed instead of V_{corr}, the theoretical value of τ changed to 570 psec. For this reason the self-consistent calculations of the screening charge distribution at the surface, performed beyond the WDA, are desired.

It should be noted here that the calculations of the positron-annihilation rate and binding energy performed in the present work are based on the WDA displaced-charge correlation function in the form (15a), in contrast to Ref. 18. The essential difference, however, consists in the fact that the electron density used in the present work was based on individual electron wave functions $\psi_{\mathbf{k}}^0(\mathbf{r})$ [obtained self-consistently according to Eqs. (20a) and (21a)–(21c)], while in Ref. 18 the parametrized form of $n_{\text{el}}(\mathbf{r})$ was applied. For this reason Jensen and Walker were not able to calculate reliable surface ACAR spectra (cf. discussion in Refs. 15 and 16).

The forms (20a) and (20b) of the electron and positron wave functions employed in the WDA ACAR formula (19) lead to the expressions for 1D SS ACAR spectra

$$\rho(p_z) = 2\pi \int_0^{k_F} (k_F^2 - k_z^2)\, dk_z \left| \int_{-\infty}^{\infty} e^{ip_z z} \psi_{k_z}(z) \psi_+(z) \{1 + a^3 [n^*(z)]/[8\pi n^*(z)] dz\}^{1/2} \right|^2 \tag{23a}$$

and

$$\rho(p_x)=2\int_0^{(k_F^2-p_x^2)^{1/2}}(k_F^2-p_x^2-k_z^2)^{1/2}dk_z\int_{-\infty}^{\infty}|\psi_{k_z}(z)|^2|\psi_+(z)|^2\{1+a^3[n^*(z)]/[8\pi n^*(z)]\}dz\ . \tag{23b}$$

The momentum distributions $\rho(p_z)$ and $\rho(p_x)$ are presented in Fig. 4(b) by solid and dashed lines, respectively. Their quasi-IPM analogs, obtained according to formulas (23) with $a^3(n^*)\equiv 0$ [see also Eq. (13a)], $\rho_q^{\rm IPM}(p_z)$, and $\rho_q^{\rm IPM}(p_x)$, are given in Fig. 1(a) for comparison. Momenta are expressed in units of the Fermi momentum k_F (for Al, $k_F=6.76$ mrad) and the spectra are normalized to the same peak height. The experimental spectrum $N_{\rm exp}(p_z)$ (Ref. 4) is shown in both parts of Fig. 4 by a dotted line (the core electron contribution is not subtracted). It should be remembered that the SS part of experimental ACAR spectra from an Al surface reported in Ref. 4 was isotropic and face independent,[4] and therefore $N_{\rm exp}(p_z)$ for Al(100) may be treated as representative of 1D SS distributions from three low-index Al surfaces.

It is apparent that including electron-positron correlations causes narrowing of theoretical ACAR spectra and both reverses and decreases the anisotropy with respect to the quasi-IPM. The agreement between theory and experiment is appreciably improved when electron-positron correlations are taken into account in the ACAR formulas (23). The full widths at half maximum (FWHM's) of $\rho(p_z)$ and $\rho(p_x)$, equal to 6.69 and 6.84 mrad, respectively, are intermediate between the experimental isotropic results 7.1 mrad (Ref. 3) and 6.3 mrad (Ref. 4). The density $\rho(\mathbf{p})$ is isotropic within 2% with $\rho(p_z)$ narrower than $\rho(p_x)$. The latter is in agreement with Ref. 3, but in disagreement with the more recent results of Ref. 4. This fact could be attributed to the same reasons as those responsible for differences between theoretical and experimental positron lifetimes and binding energies. The discrepancies between theoretical and experimental ACAR spectra are pronounced for momenta close to the Fermi momentum and higher. This is obviously the result of neglect of lattice and core effects when the jellium model of the real Al surface is considered. I suppose that the information about the surface defects and imperfections as well as about the lattice and core effects is contained rather in the high-momentum component (HMC) of the spectrum. This is an interesting problem for further investigation. The supposed positron trapping at the surface defects[12] is unlikely to be a serious reason for reported features of experimental SS annihilation characteristics, $N_{\rm SS}(p_x,p_z)$ and λ.[3,4,10]

Because of electron-positron correlations, the MD $\rho(\mathbf{p})$ (which is measured experimentally) differs from the theoretical quasi-IPM distribution $\rho_q^{\rm IPM}(\mathbf{p})$ by a factor $\epsilon_{\rm MD}(\mathbf{p})$. Since quasi-IPM ACAR spectra are anisotropic, it seems to be more reasonable to consider two separate parameters $\epsilon_{\rm MD}(p_z)=\rho(p_z)/\rho_q^{\rm IPM}(p_z)$ and $\epsilon_{\rm MD}(p_x)=\rho(p_x)/\rho_q^{\rm IPM}(p_x)$, instead of one isotropic $\epsilon_{\rm MD}(|\mathbf{p}|)$, often used in the case of bulk metal.

In Fig. 5 the values of $\epsilon_{\rm MD}(p_z)/\epsilon_{\rm MD}(p_z=0)$ and $\epsilon_{\rm MD}(p_x)/\epsilon_{\rm MD}(p_x=0)$, presented by solid and dashed lines, respectively, are compared with the "experimental" enhancement factor $\epsilon_{\rm expt}(p_z)/\epsilon_{\rm expt}(p_z=0)$ extracted from Ref. 4 (dotted line), where $\epsilon_{\rm expt}(p_z)=N_{\rm expt}(p_z)/\rho_q^{\rm IPM}(p_z)$. A reasonable agreement between $\epsilon_{\rm MD}(p_z)$ and $\epsilon_{\rm expt}(p_z)$ is observed. Both $\epsilon_{\rm MD}(p_x)$ and $\epsilon_{\rm MD}(p_z)$ are decreasing functions of momentum. This is a surprising feature because in the bulk metal the enhancement factors for valence electrons are always increasing functions of momentum as well as because local electron-positron correlations approximated by $f(\mathbf{r},\mathbf{k})=1+\Delta\rho(\mathbf{r},\mathbf{r})/n_{\rm el}(\mathbf{r})$ are momentum independent. On the other hand, this decrease of the surface $\epsilon_{\rm MD}(\mathbf{p})$ is in agreement with experimental data: Any of the calculated quasi-IPM ACAR spectra[11,12] is broader than the experimental ones[4] and therefore results of this work cannot be attributed to the method of calculation of the electron and positron wave

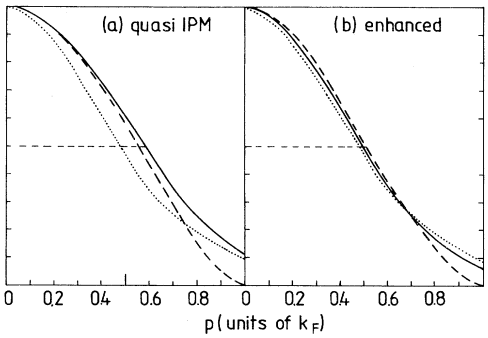

FIG. 4. 1D ACAR spectra from an Al surface calculated within (a) the quasi-IPM [Eq. (13a)] and (b) according to formulas (23). Directions perpendicular and parallel to the surface are denoted by solid and dashed lines, respectively. The experimental values of the momentum density $N_{\rm expt}(p_z)$, extracted from Ref. 4, are presented by dotted lines in both parts of the figure.

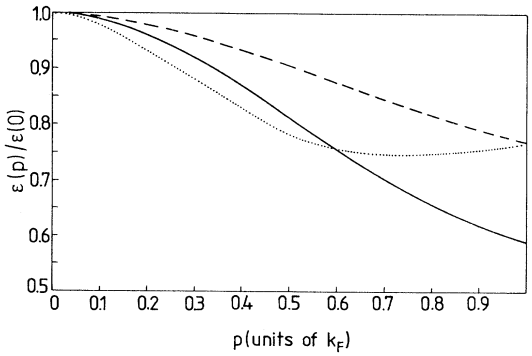

FIG. 5. Momentum-dependent enhancement factors at an Al surface, $\epsilon_{\rm MD}(p_z)/\epsilon_{\rm MD}(p_z=0)$ (solid line) and $\epsilon_{\rm MD}(p_x)/\epsilon_{\rm MD}(p_x=0)$ (dashed line), compared with experimental values $\epsilon_{\rm expt}(p_z)/\epsilon_{\rm expt}(p_z=0)$ (dotted line), where $\epsilon_{\rm expt}(p_z)=N_{\rm expt}(p_z)/\rho_q^{\rm IPM}(p_z)$ is extracted from Ref. 4.

functions alone. Moreover, for core and d electrons in a series of bulk metals, the negative slope of $\epsilon_{MD}(\mathbf{p})$ was found as well.[20,28]

$\epsilon_{MD}(p_z)$ shows a stronger tendency to decrease than $\epsilon_{MD}(p_x)$. The behavior of experimental enhancement factors is similar to the theoretical one. In my opinion the stronger decrease of experimental $\epsilon_{expt}(p_z)$ at an Al surface is common for all quasi-IPM calculations because experimental ACAR spectra are isotropic[3,4] while for any theoretical quasi-IPM densities[11,12] the parallel component is narrower than the perpendicular one.

IV. CONCLUSIONS

In the present work the effect of electron-positron correlations at the metal surface on the theoretical positron surface-state annihilation characteristics is emphasized. The interdependence between the distortion of the electron background charge density and positron distribution is set forth. It is pointed out that the positron lifetime τ and momentum density of annihilating pairs $\rho(\mathbf{p})$ cannot be considered separately, as it is done, e.g., in Ref. 11. The well-known expression for a total annihilation rate [Eq. (3b)] (Refs. 2, 21, and 29) is derived directly from the ACAR formula (3a) and definition of screening charge distribution (2a). Electron-positron correlations are treated within the proposed formalism in a consistent way.

The momentum density of annihilating pairs is calculated according to the ACAR formula (5). It should be stressed here that the approximation (5) of the exact ACAR expression (1a) or (3a), which is valid at the metal surface, must be treated with a great deal of caution in the bulk material, where state selectivity of the pair correlation functions $f(\mathbf{r},i)$ is of major importance.[19,28(a),28(b)] The annihilation parameters obtained within the proposed approach are found to be in fairly good agreement with Al experimental data,[1(a),1(d),4,10] in spite of the fact that the calculations were performed within the jellium model of an ideal Al surface. Inclusion of electron-positron enhancement effects into the ACAR and lifetime formulas appreciably improves the agreement between theory and experiment in comparison with the quasi-IPM.

Because of the nearly free nature of valence electrons in Al,[4] the deviations of parallel components of electron wave functions $\psi^0_{\mathbf{k}}(\mathbf{r})$ in the real metal from single plane waves, $S^{-1/2}e^{i(k_x x+k_y y)}$, assumed within the model of jellium, is much less pronounced in the resulting SS annihilation characteristics than electron-positron enhancement effects. In contrast to the electron and positron distributions parallel to the surface, the normal components of the electron wave functions $\psi_{k_z}(z)$ have an essential influence on the theoretical positron lifetime and ACAR spectra in Al. It should also be noted here that for d-electron metals (e.g., for copper) the jellium model of the surface is far from being satisfactory and band-structure calculations are necessary. The energy distribution near the Fermi energy is also decisive in the momentum density of the Ps emission from metal surfaces,[1(a),4] and therefore the electron-gas model is also not adequate in the interpretation of Ps ACAR spectra, in contrast to the SS component in simple metals.

Electron-positron enhancement factors $\epsilon_{MD}(\mathbf{p})$ at an Al surface appear to be decreasing functions of momentum, in contrast to their behavior in bulk Al. Anisotropy of $\epsilon_{MD}(\mathbf{p})$ is observed. $\epsilon_{MD}(p_z)$ exhibits a stronger tendency to decrease than $\epsilon_{MD}(p_x)$. These features of $\epsilon_{MD}(\mathbf{p})$ are in agreement with experimental results with respect to any published quasi-IPM calculations.[11,12]

The weighted-density approximation employed in the present work for modeling positron distribution and electronic screening charge density at an Al surface gives the correct account of electron-positron correlation energy in the average. Electron density on the positron, which is correctly reproduced within the WDA for a positron located well inside the metal, is overestimated for positron positions far in the vacuum and therefore must be slightly underestimated in the immediate vicinity of the surface plane. In order to determine electron-positron interactions at the surface exactly, first of all, self-consistent calculations of the screening charge distribution $\Delta\rho(\mathbf{r}_e;\mathbf{r}_p)$, performed beyond the WDA, are necessary. This is, however, still an open problem.

ACKNOWLEDGMENTS

I am grateful to Jerzy Lach for providing me with numerical values of electron wave functions as well as for his valuable help in the numerical calculations. I would like to thank Dr. Kelvin Lynn and Dr. Lie Ping Chan for the experimental data of $N_{expt}(p_x)$ and $N_{expt}(p_z)$, kindly made accessible.

[1]For reviews, see, e.g., (a) A. P. Mills, Jr., in *Positron Solid State Physics,* edited by W. Brandt and A. Dupasquier (North-Holland, Amsterdam, 1983), p. 432; (b) K. G. Lynn, *ibid.,* p. 609; (c) A. Dupasquier and A. Zecca, Riv. Nuovo Cimento **8**, 1 (1985); (d) A. P. Schultz and K. G. Lynn, Rev. Mod. Phys. **60**, 701 (1988), and references cited therein.

[2]For reviews, see, e.g., R. N. West, *Positron Studies of Condensed Matter* (Taylor & Fancis, London, 1974); S. Berko, in Ref. 1(a), p. 64; S. Berko, in *Mometum Densities,* edited by R. N. Silver and P. E. Sokol (Plenum, New York, 1989), p. 273.

[3]K. G. Lynn, A. P. Mills, Jr., R. N. West, S. Berko, K. F. Canter, and L. O. Roelling, Phys. Rev. Lett. **54**, 1702 (1985); K. G. Lynn, A. P. Mills, Jr., L. O. Roelling, and M. Weber, in *Electronic and Atomic Collisions,* edited by D. C. Lorenz, W. E. Meyerhof, and J. R. Peterson (North-Holland, New York, 1986), p. 227.

[4]D. M. Chen, S. Berko, K. F. Canter, K. G. Lynn, A. P. Mills, Jr., L. O. Roelling, P. Sferlazzo, M. Weinert, and R. N. West, Phys. Rev. Lett. **58**, 921 (1987); Phys. Rev. B **39**, 3966 (1989).

[5]R. H. Howell, P. Meyer, I. J. Rosenberg, and M. J. Fluss, Phys.

Rev. Lett. **54**, 1698 (1985).
[6]D. M. Chen, Ph.D. thesis, City University of New York, 1987.
[7]P. Sferlazzo, S. Berko, K. F. Canter, D. M. Chen, K. G. Lynn, A. P. Mills, Jr., L. O. Roelling, A. Viescas, and R. N. West, Bull. Am. Phys. Soc. **32**, 899 (1987).
[8]R. H. Howell, I. J. Rosenberg, P. Meyer, and M. J. Fluss, Phys. Rev. B **35**, 4555 (1987).
[9]P. Sferlazzo, S. Berko, K. F. Canter, K. G. Lynn, A. P. Mills, Jr., L. O. Roelling, A. Viescas, and R. N. West, Phys. Rev. Lett. **60**, 538 (1988).
[10]K. G. Lynn, W. E. Frieze, and P. J. Schultz, Phys. Rev. Lett. **52**, 1137 (1984).
[11]B. Rozenfeld, W. Świątkowski, and K. Jerie, Acta. Phys. Pol. A **64**, 93 (1983); Lou Yongming, Phys. Rev. B **38**, 9490 (1988); Yongming Lou, Binglin Gu, Jialin Zhu, Chang Lee, and Jiajiong Xiong, J. Phys. Condens. Matter **1**, 2977 (1989).
[12]A. P. Brown, A. B. Walker, and R. N. West, J. Phys. F **17**, 2491 (1987); A. P. Brown, K. O. Jensen, and A. B. Walker, *ibid.* **18**, L141 (1988).
[13]R. M. Nieminen, M. J. Puska, and M. Manninen, Phys. Rev. Lett. **53**, 1298 (1984); R. M. Nieminen and M. J. Puska, *ibid.* **50**, 281 (1983).
[14]P. M. Platzman and N. Tzoar, Phys. Rev. B **33**, 5900 (1986).
[15]A. Rubaszek and J. Lach, J. Phys. Condens. Matter **1**, 9243 (1989); Surf. Sci. **211/212**, 227 (1989).
[16]A. Rubaszek, J. Phys. Condens. Matter **1**, 2141 (1989).
[17]J. E. Inglesfield and M. J. Stott, J. Phys. F **10**, 253 (1980).
[18]K. O. Jensen and A. B. Walker, J. Phys. F **18**, L277 (1988).
[19]S. Daniuk, G. Kontrym-Sznajd, A. Rubaszek, H. Stachowiak, J. Mayers, P. A. Walters, and R. N. West, J. Phys. F **17**, 1365 (1987).
[20]S. Daniuk, M. Šob, and A. Rubaszek, Phys. Rev. B **43**, 2580 (1991).
[21]A. Rubaszek and H. Stachowiak, Phys. Rev. B **38**, 3846 (1988).
[22]H. Stachowiak, Phys. Rev. B **41**, 12 522 (1990).
[23](a) P. Hohenberg and W. Kohn, Phys. Rev. **136**, B864 (1964); (b) W. Kohn and L. J. Sham, *ibid.* **140**, A1133 (1965); (c) B. Chakraborty and W. Siegel, Phys. Rev. B **27**, 4535 (1983); (d) E. Boroński and R. M. Nieminen, *ibid.* **34**, 3820 (1986); (e) H. Stachowiak and J. Lach (unpublished).
[24]O. Gunnarson, M. Johnson, and B. I. Lundqvist, Phys. Rev. B **20**, 3136 (1979).
[25]D. N. Lang, in *The Density-Functional Formalism and the Electronic Structure of Metal Surfaces,* Vol. 28 of *Solid State Physics,* edited by H. Ehrenreich, F. Seitz, and D. Turnbull (Academic, New York, 1973), p. 225.
[26]A. Kallio, P. Pietiläinen, and L. Lantto, Phys. Scr. **25**, 943 (1982).
[27](a) M. K. Harbola and V. Sahni, Phys. Rev. Lett. **62**, 489 (1989); (b) Phys. Rev. B **39**, 10 437 (1989).
[28](a) S. Daniuk, J. Phys. Condens. Matter **1**, 5561 (1989), and references cited therein; (b) S. Daniuk, G. Kontrym-Sznajd, J. Majsnerowski, H. Stachowiak, and M. Šob, *ibid.* **1**, 6321 (1989); (c) A. K. Singh, A. A. Manuel, T. Jarlborg, Y. Mathys, E. Walker, and M. Peter, Helv. Phys. Acta **59**, 410 (1986).
[29]J. Arponen and E. Pajanne, Ann. Phys. (N.Y.) **121**, 343 (1979).
[30]N. W. Ashcroft and N. D. Mermin, *Solid State Physics* (Holt, Reinhart and Wilson, New York, 1976).
[31]W. Brandt and J. Reinheimer, Phys. Lett. **35A**, 109 (1971).
[32]D. Pines, *Elementary Excitations in Solids* (Benjamin, New York, 1963).
[33](a) M. Manninen, R. Neiminen, P. Hautojärvi, and J. Arponen, Phys. Rev. B **12**, 4012 (1975); (b) R. Monnier and J. P. Perdew, *ibid.* **17**, 2595 (1978).
[34](a) V. Heine and C. H. Hodghes, J. Phys. C **5**, 225 (1975); (b) O. V. Boev, M. J. Puska, and R. Nieminen, Phys. Rev. B **36**, 7786 (1987); (c) J. P. Perdew, H. Q. Tran, and E. D. Smith, *ibid.* **42**, 11 627 (1990).
[35]D. N. Lang and W. Kohn, Phys. Rev. B **3**, 1215 (1971).
[36]S. Berko and J. Plaskett, Phys. Rev. **112**, 1877 (1958); C. H. Hodges, Phys. Rev. Lett. **25**, 284 (1970); C. H. Hodges and M. J. Stott, Phys. Rev. B **1**, 73 (1973); R. M. Nieminen and C. H. Hodges, Solid State Commun. **18**, 1115 (1976).
[37]R. M. Nieminen and K. O. Jensen, Phys. Rev. B **38**, 5764 (1988).